Surface topography in machining Ti alloys for biomedical applications: Correlative microscopy approach for qualitative and quantitative analysis

Sílvia Carvalho, Ana Horovistiz*, J. Paulo Davim

Department of Mechanical Engineering, Centre for Mechanical Technology and Automation Engineering -TEMA- University of Aveiro, Campus Santiago, 3810-193, Aveiro, Portugal

*Corresponding author. Tel.: +351 234 370 830. E-mail address: horovistiz@ua.pt

Abstract:

V-Free Ti-6Al-7Nb alloy may be an interesting candidate as a substitute to the traditional Ti-6Al-4V alloy on development of biomedical components. The inspection of surface integrity through digital microscopy techniques shows strong potential for comparative analysis and optimization of manufacturing processes. This work deals with the comparative analysis of turned surfaces of dual-phase (α+β) titanium alloys: Ti-6Al-4V and Ti-6Al-7Nb, under different cutting conditions. Digital image processing and analysis technique has been used to evaluate the volume fraction of phases and their distribution. An innovative methodology for digitizing the surface topography was applied, based on the association of modern microscopy techniques with digital image processing-Correlative Microscopy. The global outcomes show that Ti-6Al-4V samples presented better homogeneity, with a mean β volume fraction of about 17%, compared to 11% of Ti-6Al-7Nb samples. Combination of higher feed rate and lower velocity produce rougher topography for both alloys, while the topographic formation obtained by the combination of lower feed rate and higher velocity seems smoother. In addition, Ti-6Al-4V alloy presents rougher topography in comparison topography of Ti-6Al-7Nb, under all conditions, probably due to the different phase distribution. The correlative microscopy allowed a correspondence between the cutting conditions and the microstructural properties of the both Ti-6Al-4V and Ti-6Al-7Nb alloys, through the analysis of the machined surface.

Keywords: Surface topography; Microstructural aspects; Correlative microscopy; Cutting conditions; Machining of titanium alloys

1. Introduction

Production by CNC machining plays an important role in the development of biomedical components, such as, dental implants, prosthesis, and artificial joints. There are specific requirements concerning the properties of the selected materials and the manufacturing processes to obtain them. The material must have high biocompatibility, wear and corrosion resistance and suitable mechanical properties (strength, elastic modulus, fatigue resistance, fracture toughness) regarding the dysfunctional organs to be substituted. These requirements [1] are critical to avoid implant rejection due to adverse tissue reaction and premature component failure associated with high bone resorption and generation of wear debris.

Concerning the metallic biomaterials, titanium alloys are widely used to produce hard tissue replacements. Nowadays, Ti-6Al-4V, (α+β) titanium alloy is the most frequently selected alloy, due to their superior properties, such as, excellent strength-to-weight ratio, strong corrosion resistance and ability to retain high strength at elevated temperatures. Two crystal structures exist in titanium alloys after the equilibrium cooling condition, α phase (hexagonal close-packed structure, HCP) and β phase (body-centered cubic structure, BCC). In despite of this, some authors found out that Vanadium ions released from the implants could cause long-term health problems, such as Alzheimer and osteomalacia [2].

In order to overcome these limitations, new titanium alloys are developed without the presence of Vanadium, the V-Free alloys, such as Ti-6Al-7Nb, Ti-13Nb-13Zr, Ti-5Al-2,5Fe alloys, among others [3]. Ti-6Al-7Nb (α+β) titanium alloy [4] is the most frequent substitute for the vanadium alloy since niobium is bioinert and has an elastic modulus closer to the human bone.

The controlling of the surface integrity obtained after machining is crucial for functional properties of components used in all areas of industry [5], and requires different criteria regarding the technical functionality of the component in service. In the biocomponent industry, for instance, the rate and quality of osteointegration can be improved by controlling surface aspects like surface topography, subsurface deformation (inherent to material properties) and distribution of chemical elements. [6,7].

Several authors reported that the machinability of titanium alloys (α+β), in terms of surface integrity, differs accordingly with: the microstructure morphology [8,9] (coarse microstructure alloys are more difficult to cut than finer grain structures); volume fraction of β-phase [10-12] (an higher volume fraction of β phase increases the strength presented by the alloy) and distribution of phases [8,13] (both α and β phases are relatively soft but α–β interface is an effective stoppage to dislocation and crack

propagation). Machined surface integrity depends on the relationship among these microstructural aspects.

Surface topography, most of the times, is evaluated by techniques that involve stylus-based roughness measurements. These assessments are often carried out by analyzing 2D parameters that describe vertical deviations from the surface. Ra is one of the most used, and it is obtained by calculating the deviation of the roughness profile from the center line of the profile. Other roughness parameters are more robust to find specific deviation, such as the maximum peak-to-valley height (Rt) and the average maximum peak-to-valley height (RzD), which is obtained considering the average value of smaller samples within the evaluation length. Some authors refer to the importance of analyzing several roughness parameters for a better description and quantification of the roughness profile [14]. Nevertheless, the surface functionality has a dependence on the machined layers because these influence the surface texture anisotropy [15]. The characterization of the surface topography in terms of 3D parameters has thus an enhanced relevance relatively to 2D surface finish parameters.

Extraction of surface topography information of machined materials can be obtained by quantitative microscopy. These approaches can quantitatively relate the 3D complexes topographic patterns of the machined surfaces to the cutting parameters and properties of the materials: It is the case of topography analysis through recognized fractal dimension approach [16]. On the other hand, the complete inspection of surface relief should be correlated with concepts, such as: 3D reconstruction of the surface texture and association of techniques capable of providing a wide range of information on topography patterns, combined with chemical modifications related with microstructural aspects. This analysis would be of great value for the industry of biocomponents, since these parts have very strict requirements of the surface topography patterns associated with their chemical functionality.

In this respect, correlative microscopy [17] is advantageous and may replace the conventional analysis techniques, as it improves the general comprehension of simultaneous phenomena associated with the formation of machined surfaces. This method consists of inspecting the same field using different microscopy techniques. One of the microscopy methodologies contributes to the topographical interpretation of surface, while another provides qualitative/quantitative information about some property for the same sample region. The association of scanning electron microscope (SEM) [18] with the optical microscopy (OM) [19] have been proposed for evaluation of microstructures in terms of a large range of surface properties [17]. This technique has been recently successfully for inspection of the machined surface of Ti-6Al-7Nb samples [20].

The main objective of this work was to evaluate, comparatively, the integrity of machined surfaces of the Ti-6Al-4V and Ti-6Al-7Nb titanium alloys. The machined surfaces were obtained in dry

turning operations, with certain set cutting conditions. An unconventional approach to inspecting the integrity of machined surfaces is presented: the correlative microscopy. This technique was based on the association of reconstruction of surfaces [16] based on digital processing of images obtained by OM with SEM and microanalysis modes (Energy-dispersive X-ray spectroscopy-EDS). This methodology allowed a certain degree of understanding of the correspondence between the cutting conditions and microstructural aspects of the titanium alloys, through the analysis of the machined surface since shows modifications in the distribution of the chemical elements present in the alloy in preferential sites, related to the machining topographies patterns.

2. Materials and methods

2.1 Microstructural characterization

Microstructural characterization was conducted using bars (diameter of 12mm) of Ti-6Al-4V and Ti-6Al-7Nb titanium alloys produced by TiFast S.r.l. Both Ti alloys are α+β duplex phases titanium alloy, no coarse, elongated α platelets and inclusion free. The alloys were extruded and then been subjected to heat treatment for stress relief annealing. Table 1 presents the chemical properties of the materials. Cylindrical bar samples of each titanium alloy (approximately 5 mm of thickness) were sectioned using an abrasive cutting wheel machine with lubrication. The cross-section of both samples was ground using a sequence of grinding paper and polished with a cloth containing a diamond suspension. Polished surfaces were etched by immersion in Kroll's reagent for 20 seconds.

Polished and chemically etched surfaces were observed by MO (Nikon-Eclipse LV150 reflected Optical microscope) and SEM with EDS inspection (Hitachi TM400Plus). Digital image processing routines were applied to inspect the microstructural features, namely, the volume fraction of β phases and their dispersion along the transversal section accordingly the sampling scheme showed on Fig.1.

Vickers microhardness tests were performed on samples of each alloy. The load applied was 2N during 10s. Five indentations were made along the cross-sections for every sample. The values presented are the averages of the values collected.

Table 1 Chemical composition in % atomic weight for Ti-6Al-7Nb and Ti-6Al-4V

Ti-6Al-7Nb (ASTM F1295)								
Al	C	Fe	H	N	Nb	O	Ta	Ti
5.82 5.83	0.021 0.024	0.10 0.11	0.003	0.010	6,81 6,87	0.155 0.164	0,014	Balance
Ti-6Al-4V (ASM 4928)								
Al	C	Fe	H	N	V	O		Ti
5.92 5.94	0.023 0.024	0.1	0.005	0.006	3.84 3.86	0.110 0.112	0.005	Balance

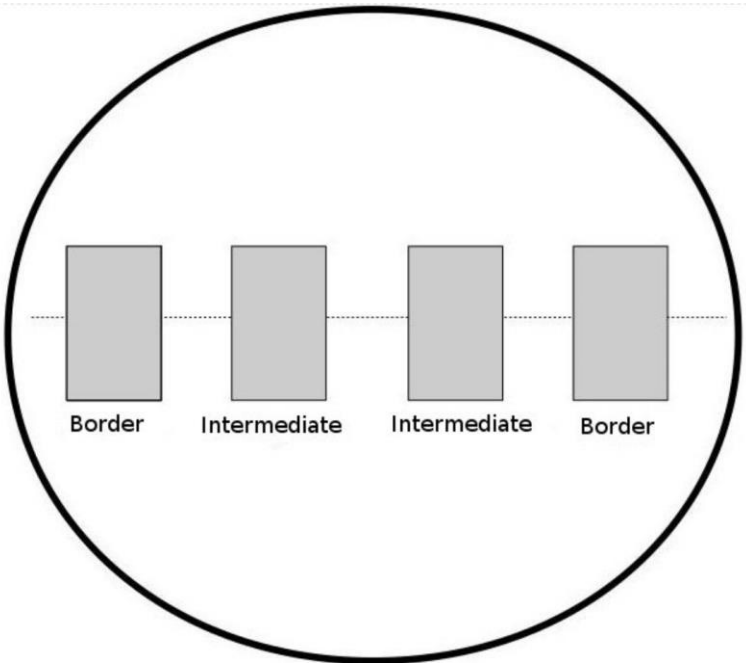

Fig.1 Scheme of microstructural inspection of samples of Ti alloys.

2.2 Machining experiments

Cylindrical bar samples of Titanium alloys, Ti-6Al-4V and Ti-6Al-7Nb were employed in the machining experiment. An external turning operation was performed in Ti-6Al-4V and Ti-6Al-7Nb samples with a Kingsbury MHP 50 CNC turning center. The (Ti, Al)N + TiN coated cutting inserts with a designation, CNMG 120408-MF1 TS200 were placed in a tool holder (C3-PCLNL-22040-12) that was attached in the turning center turret. The machining conditions for the experiments are listed in Table 2, where v_c is the cutting speed, f is the feed rate and a_p is the depth of cut. All the experiments were made under dry condition. The samples were then analyzed using the correlative microscopy method.

Table 2 Cutting parameters for turning operations.

Sample designation	Alloy designation	V_c [m/min]	f [mm/rev]	a_p [mm]	Cutting length [mm]
V1	Ti-6Al-4V	30	0.15	0.5	6
V2		90	0.05		
N1	Ti-6Al-7Nb	30	0.15		
N2		90	0.05		

Roughness values were measured with a Hommel Tester T1000 roughness tester. For each workpiece, ten measurements were carried out on the surface. At each measurement position, Ra, Rt and RzD roughness parameters were acquired.

2.3. Surface topography analysis: correlative microscopy analysis

Samples with approximately 5 mm were sectioned from the main turning samples, one for each condition presented at Table2. Then, the sample was placed in an aluminium bidimensional scaled sample holder, developed for this experiment as shown in Fig.2. This configuration (tool holder + sample) was maintained during all steps of the analysis. The complete description of the procedure is reported elsewhere [17].

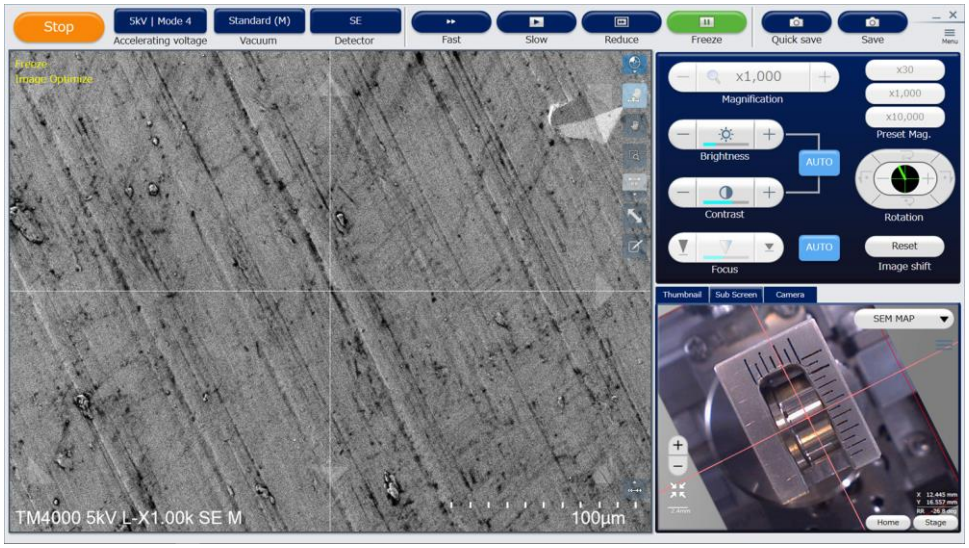

Fig.2 Example of SEM placement. In the right corner is tool holder + sample.

3 Results and discussion

3.1 Microstructural and structural aspects of Ti-6Al-4V and Ti-6Al-7Nb alloys

The results of microstructural characterization of as-received materials are exhibited on the sequence in Fig.3-7. Fig.3 exhibits the micrographs, obtained by OM, with the respective microstructure of Ti-6Al-4V (a) and Ti-6Al-7Nb (b) alloys. It is possible to observe that both structures they seem composed of a fine dispersion of α and β phases without elongated or acicular α phases.

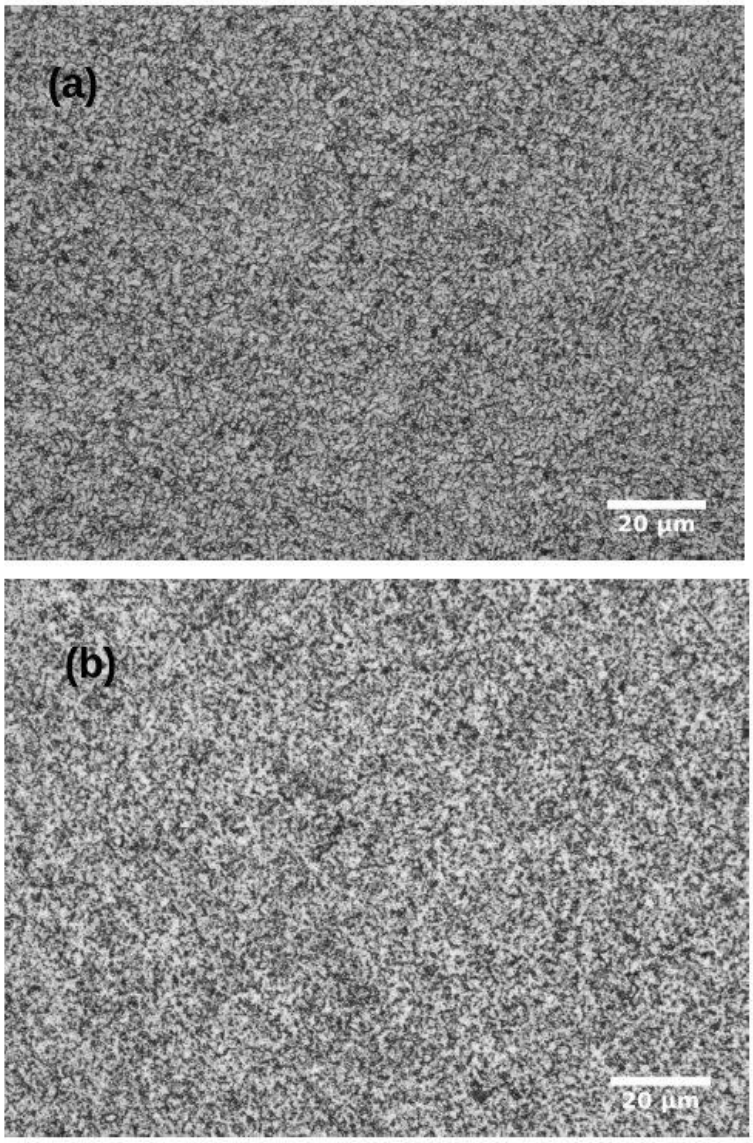

Fig.3 Microstructures obtained in optical microscopy in samples of the composition of Ti-6Al-4V (a) and Ti-6Al-7Nb (b).

EDS analysis was performed in order to confirm the chemical compositions of phases. SEM image of Ti-6Al-7Nb sample was taken as an example. In Fig.4 one can observe that the lighter phase is richer in Nb. In fact, accordingly to the literature [19], β phase is rich in β stabilizers, such as Nb, V, Mn, and Cr, while α phase is rich in α stabilizers. such as Al, O, N.

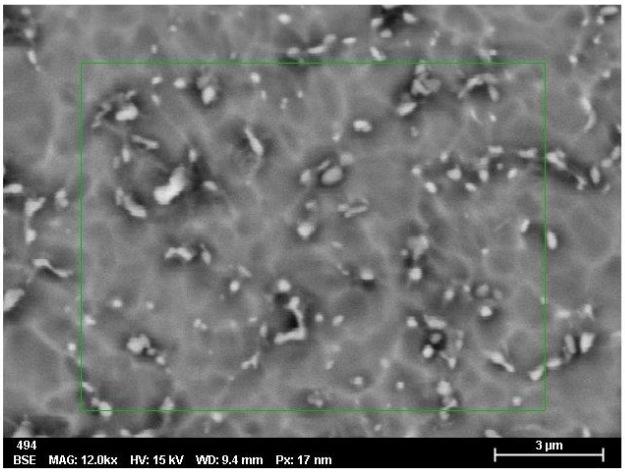

Name	Date	Time	HV [kV]	Mag	WD [mm]
494	1/25/2019	5:17:44 PM	15.0 keV	12000x	9.4 mm

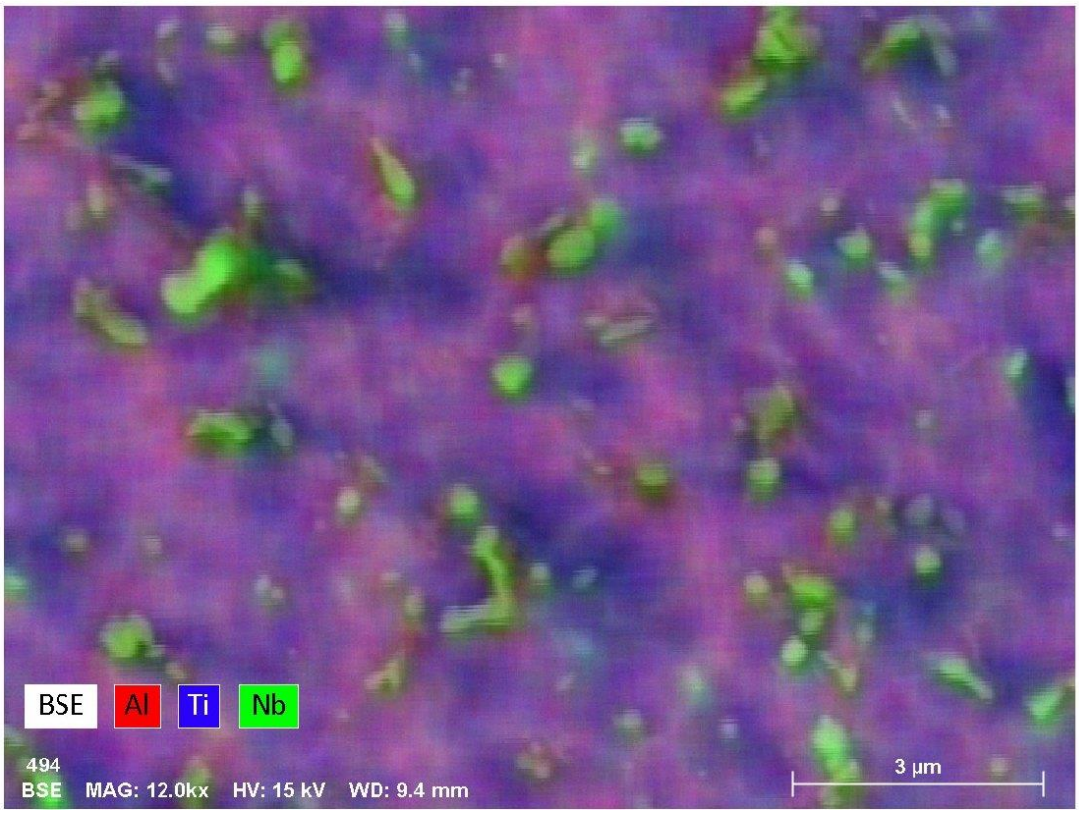

Fig.4 EDS map of chemical element distribution for sample of Ti-6Al-7Nb. Red, blue and green colors are representing, respectively, the distribution of Ti, Nb, and Al.

Fig.5 exhibits examples of microstructures of the both Ti-6Al-4V and Ti-6Al-7Nb alloys obtained by electronic microscopy where two well-defined biphasic structures can be observed. One can note the presence of the β phase (lighter) distributed in a darker matrix α. This distribution looks like distinct in

the two alloys, Ti-6Al-4V (Fig. 5a) and Ti-6Al-7Nb (Fig. 5b). In Ti-6Al-4V alloy, the lighter phase (β phase) concentrates on the grain boundaries (Fig. 5a), while in Ti-6Al-7Nb (Fig. 5b) shows that the lighter phase has a more concentrated distribution.

The Fig.6 shows an assembly of microstructures taken along the cross-section of samples from the Ti-6Al-4V and Ti-6Al-7Nb alloys, according to the scheme of Fig.1. The average Vickers microhardness values for each material are also presented in this image.

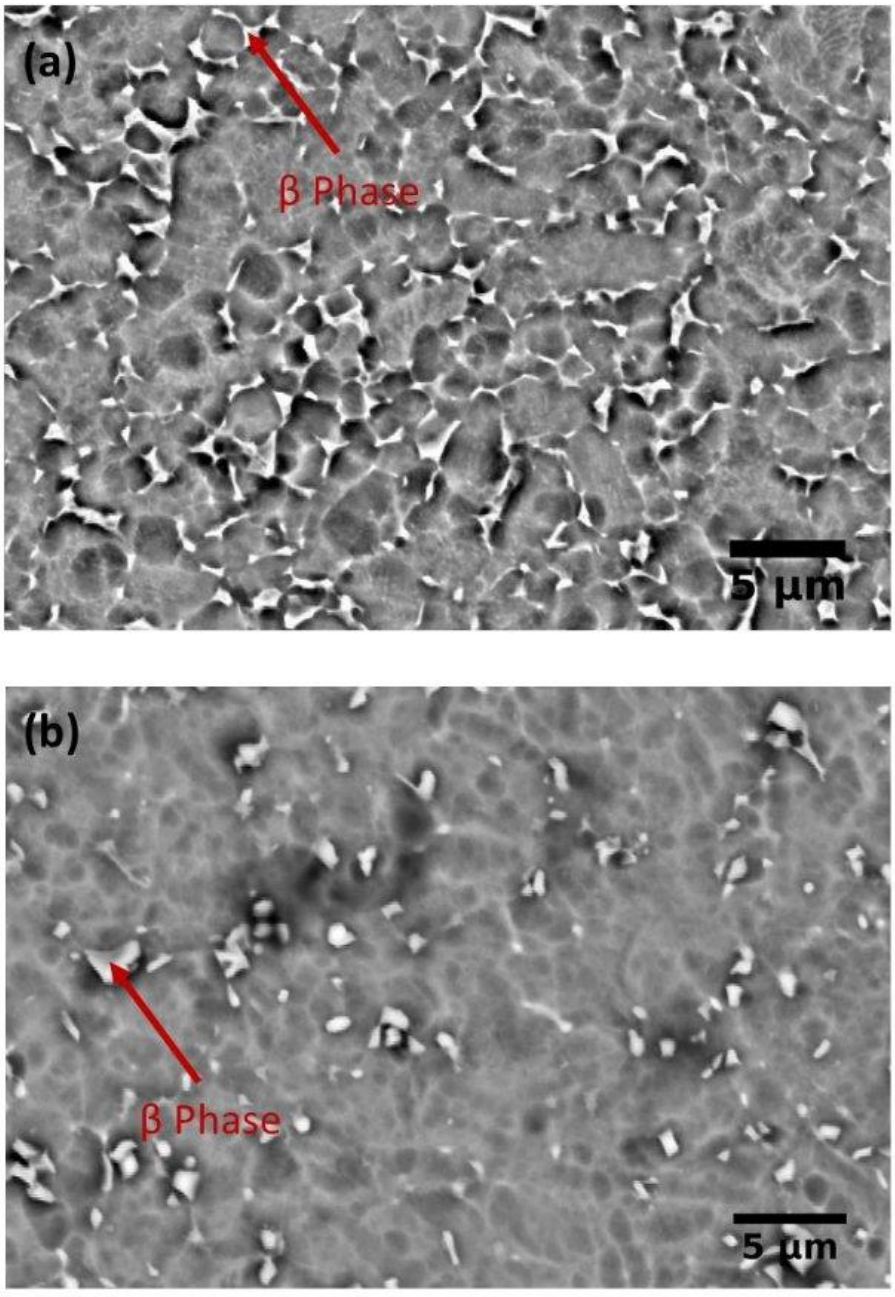

Fig.5 Microstructures obtained by scan electron microscopy for samples of two Ti-alloys, Ti-6Al-4V (a) and Ti-6Al-7Nb (b).

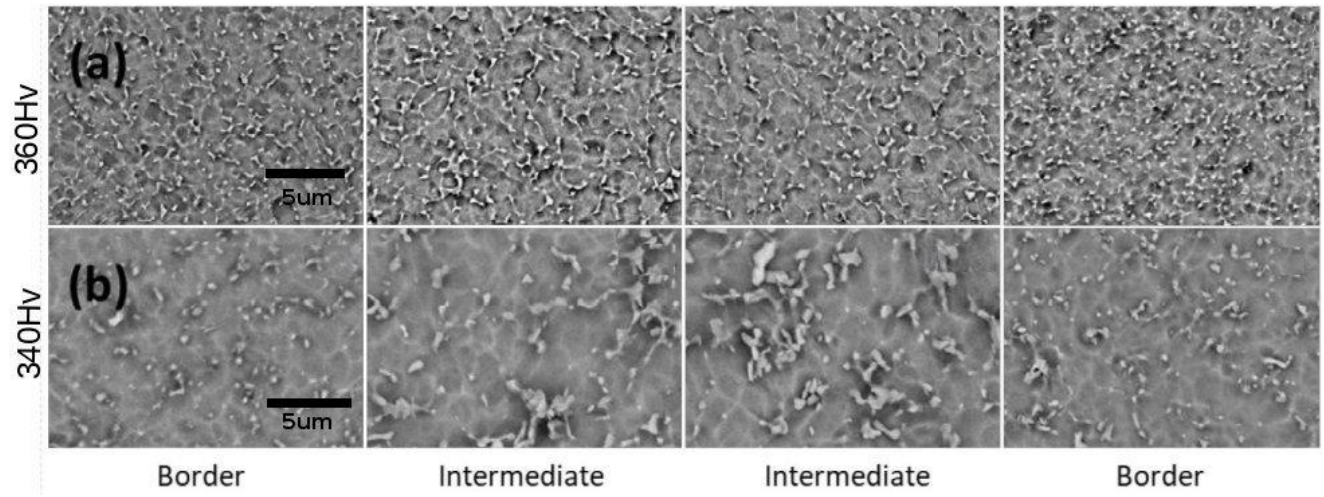

Fig.6 Assembly of the micrographic inspection taken along the cross-section for the two alloys Ti-6Al-4V (a) and Ti-6Al-7Nb (b). with their respective average Vickers microhardness values, performed according to the scheme of Fig. 1.

The quantitative analysis of the beta phase fraction and its dispersion in the α matrix for the two Ti alloys is shown in Fig.7. First, the images were binarized (Fig.7a shows an example of micrography taken from a sample of Ti-6Al-4V with its respective binary image, Fig. 7b). Then these images were divided into squares of width 100 pixels. The ratio of black pixels (eg 10% black pixels = 0.1) was calculated within each square. The mean of this ratio and the respective standard deviation for each alloy are: Ti-6Al-4V (mean=0.174 std=0.0926) and Ti-6Al-7Nb (mean=0.108 std=0.1717). This process was repeated for other widths of the squares (boxes) and the result as shown Fig.7. The results presented in plots of Fig.7 correspond to the combination of information obtained from several microstructures, collected in different fields of each sample in order to compensate for biased sampling [20].

The mean plot (Fig.7c) confirms that the volume fraction of the Ti-6Al-4V alloy is higher compared to the Ti-6Al-7Nb alloy. Regardless of the size of the box width, the value is more or less constant (some oscillations may be due to image noises). On the other hand, the standard deviation values (Fig.8d) prove, quantitatively, that Ti-6Al-4V clearly presents a more homogeneously distributed β phase dispersion.

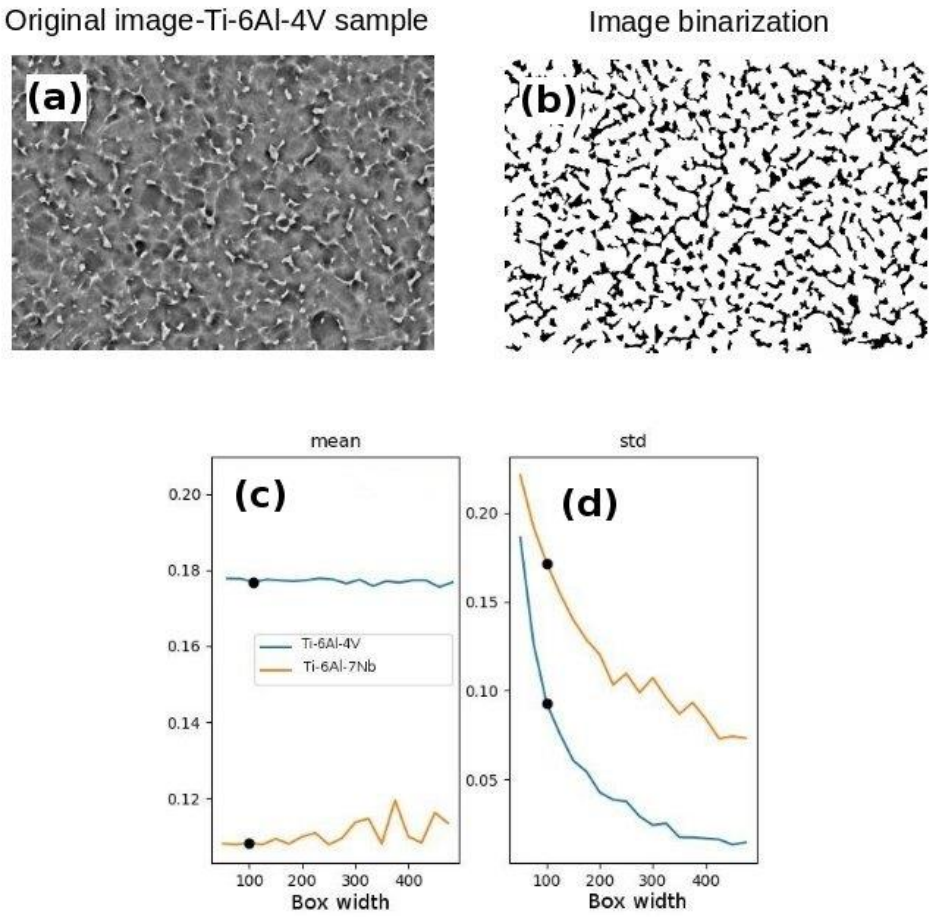

Fig.7. Example of one of the micrographs of Ti-6Al-4V, (a), with its respective binary image, (b), used for the construction of mean plots, (c), and standard deviation plot, (d), for both Ti alloys. Note: Box width=100 seems to be an adequate width as it is the order (a little bigger) of the size of the black spots in the images.

3.2 Surface analysis

Fig.8 is a montage with the data distribution of the surface roughness parameters (Ra, Rt, and RzD) for both machined materials using boxplot visualization. The boxplot graphical method can be applied when comparing different groups of samples more quantitatively since the data distribution is divided into four equal parts, each containing 25% of the data, which means that 50% of the data is represented by the box length (interquartile range, which is the difference between the upper quartile and lower quartile). This way of observing the data is quite useful to understand the aspect of dispersion and other statistical descriptors of the samples (such as median).

Correlative Microscopy combines the texture information of the machined surfaces, obtained from OM height maps to the chemical element distribution maps obtained by microanalysis in SEM

images. In addition, the aspects of topography, such as, possible inclusions and material re-deposition, can be compared between SEM/EDS and reconstructed OM images.

The overall outcomes of machined surfaces analysis are presented on the sequence of Fig.9 and 10. Fig.9. and correspond to sampling collected in random fields in each sample in order to compensate for possible heterogeneities. Fig.9 illustrate examples of SEM images, their respective surface topography and corresponding surface chemical analysis for Ti-6Al-4V (V1) and Ti-6Al-7Nb (N1), after turning tests under the same cutting conditions (Table1). Analogously, Fig.10 presents the examples of SEM images, surface topography and surface chemical analysis for both alloys, Ti-6Al-4V (V2) and Ti-6Al-7Nb (N2) after turning tests under the identical cutting conditions.

The general analysis of the results suggests that the cutting conditions affect the surface topography and chemical distribution elements of alloy samples. In Fig.9 a-b and Fig 10 a-b one can note an evolution of the feed marks according to the variation of the feed rate, *f,* (Table1). SEM images show well-defined feed marks. Those periodic marks are formed due to the mutual effect of the tool linear motion along the workpiece and the workpiece rotation.

The elevation maps of machined surfaces are shown in Fig.9 c-d and Fig.10 c-d. Apparently, machined surfaces obtained by the combination of higher feed rate and lower velocity (f=0.15 mm/rev and v_c=30m/min) produce rougher topography, with higher feed ridges, for both alloys (Fig.9 c-d), while the topographic formation described on Fig.10 c-d, obtained by the combination of lower feed rate and higher velocity (f=0.05 mm/rev and v_c=90m/min) seems smoother.

There seems to be a qualitative agreement between the roughness values measured and the topography displayed in Fig.9 a-b and Fig.10 a-b. Actually, from Fig.8 observation it is possible to see that the roughness measurements are grouped according to the cutting conditions for both machined alloys, for all surface roughness parameters. It is also remarkable that Ti-6Al-7Nb alloy samples are more sensitive to variation in cutting conditions compared to Ti-6Al-4V alloy samples (as an example, the maximum difference of Ra for Ti-6Al-7Nb is 0.54 um (0.68 um (N1) – 0.14 um (N2)), while that the maximum difference of Ra for Ti-6Al-4V is 0.47 um (0.75 um (V1) – 0.28 um (V2)).

These measurement findings are consistent with the effects of cutting condition on topography. Several studies [23-25] verified the strong influence of the feed rate on the surface finish for Ti alloys, during the turning operation, which must be kept low to provide better surface quality. On the other hand, other authors [26-28] have shown that higher values of v_c can contribute to obtaining a turned surface of Ti alloys with better quality. This phenomenon can be explained, mainly, by the effect of thermal softening of the material, which contributes to the decrease of the mechanical resistance of the part, reducing the cutting forces and facilitating the machining, and by the lesser deformation of the chip,

which tends to preserve the surface newly machined. It is from to emphasize that definition of high or low v_c is relative, taking into account the different levels adopted in the literature for this cutoff parameters.

Ti-6Al-4V alloy presents worse (rougher) topography (Fig.9a and c) in comparison topography of Ti-6Al-7Nb (Fig.10a and c). A probable explanation can be related to the differences in the microstructural aspects of both alloys, in the region of the surfaces submitted to the cutting operation (Fig.6). Recent studies suggest than the increase in β phase content in matrix α [8] and/or homogeneous distribution of β phase at the grain boundaries [29] of the equiaxed α phase can lead to increase in mechanical strength and hardness of Ti alloys. The increase in hardness and mechanical strength of Ti alloys can generate high machining forces which result in tool deformation. Beside of this, the high dynamic shear strength during the cutting operation results in localized shear stresses [30] and segmented chips that, in turn, generate dynamic cyclic forces, causing more irregular machined surfaces.

Fig.9 e-f and Fig.10 e-f depict the evolution of EDS maps in which it is one can observe a change in the homogeneity of distribution of points related to the chemical elements. These modifications are especially remarkable in Fig.9e, corresponding to condition V1 (Table1), where one can observe two stripes, apparently coincident with the feed marks developed during the turning operation. In fact, the distribution of chemical elements (Fig.11) shows that there was a depletion of the green color, corresponding to the element Al, located in these stripes, highlighting the V, represented by the color blue. Some works have reported modifications of phases and grain sizes on machined surfaces of Ti-6Al-4V titanium alloy [10, 29, 31]. The authors demonstrated that the cutting parameters, such as, cutting speed and depth of cut played a fundamental role in the microstructural transformation. It is evident that the understanding of this phenomenon will have to contemplate a global analysis of the turning process, such as temperature measurements, forces, and a detailed microstructural study, including subsurface analysis of the Ti-6Al-4V and Ti-6Al-7Nb alloys. Anyway, this is important experimental evidence, as it shows that some cutting conditions can promote the exposition of zones of concentration of V, which is toxic to the organism.

Finally, other types of surface damages can be observed on the machined surface alloy samples under different cutting conditions (Fig.9 and Fig.10). These defects can be attributed to the re-deposition of particles from the metal debris and micro-pits, due to their morphology and size [31]. There seems to be an agreement between the re-deposition material regions in the SEM images (Fig. 9a- b and Fig.10 a-b) with their respective peaks in 3D representations of the height map (Fig.9 c-d and Fig.10 c-d). Likewise, the micro-pits that can be observed in SEM images and in the corresponding regions in small valleys in 3D representation of the height map.

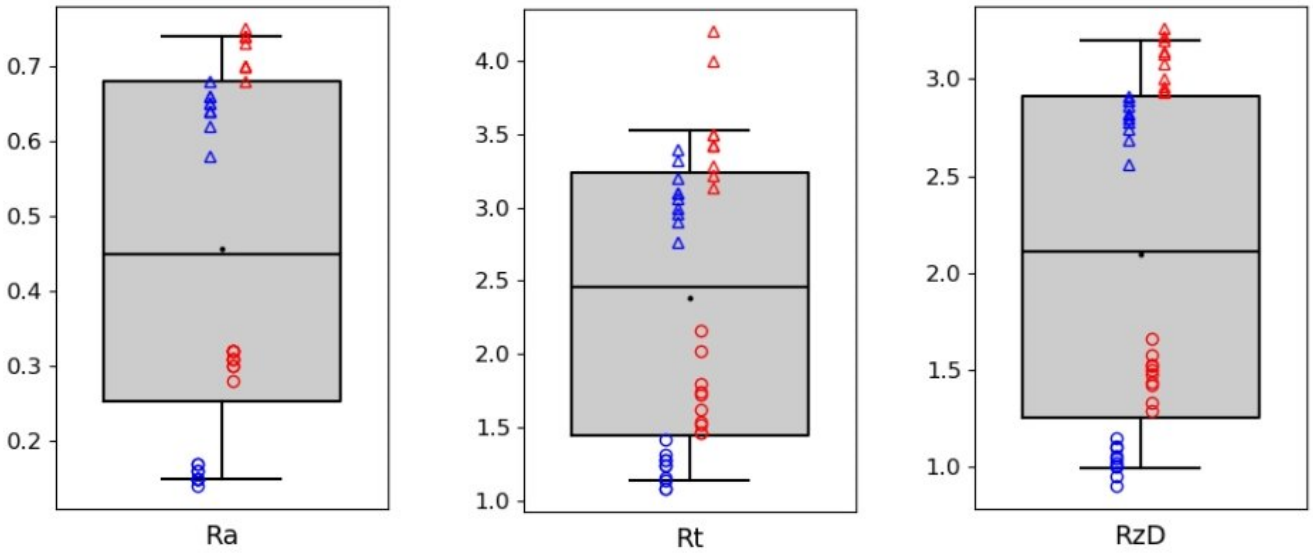

Fig.8 Boxplot visualization for data distribution of roughness parameters Ra, Rt, and RzD for both machined alloys. The following symbols are used to represent roughness measurements, taking into account Table2: Blue triangle- N1; red triangle -V1; blue circle-N2; red circle V2.

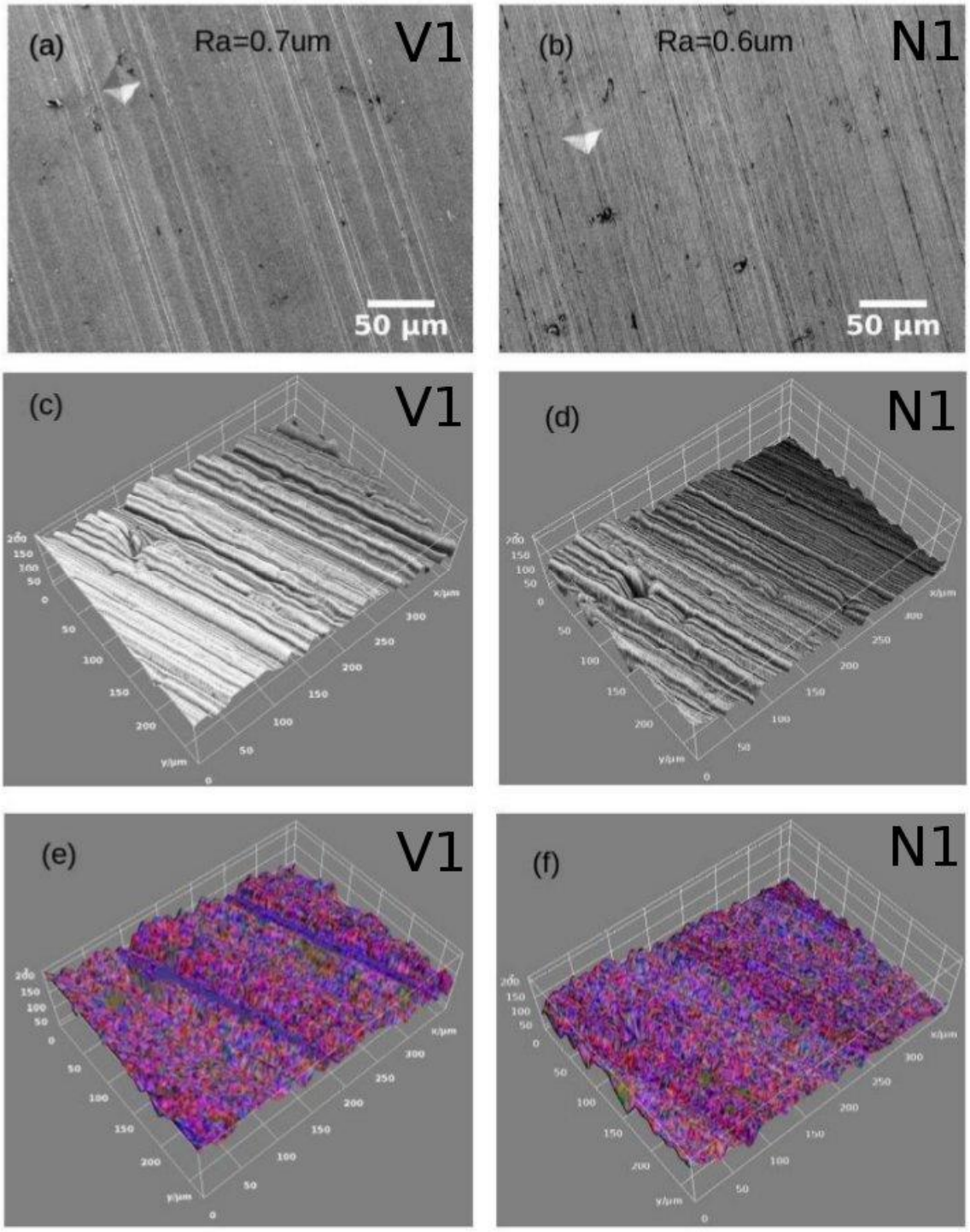

Fig.9 SEM micrographs of machined samples V1 (a) and N1 (b) and equivalent 3D elevation map for V1 (c) and N1 (d) with corresponding EDS map of V1 (e) and N1 (f) for the same cutting parameters: V c=30 m/min; f=0.15 mm/rev; a p=0.5 mm. The red, blue, green, color are representing, respectively, the distribution of Ti, V(e) or Nb (f), and Al.

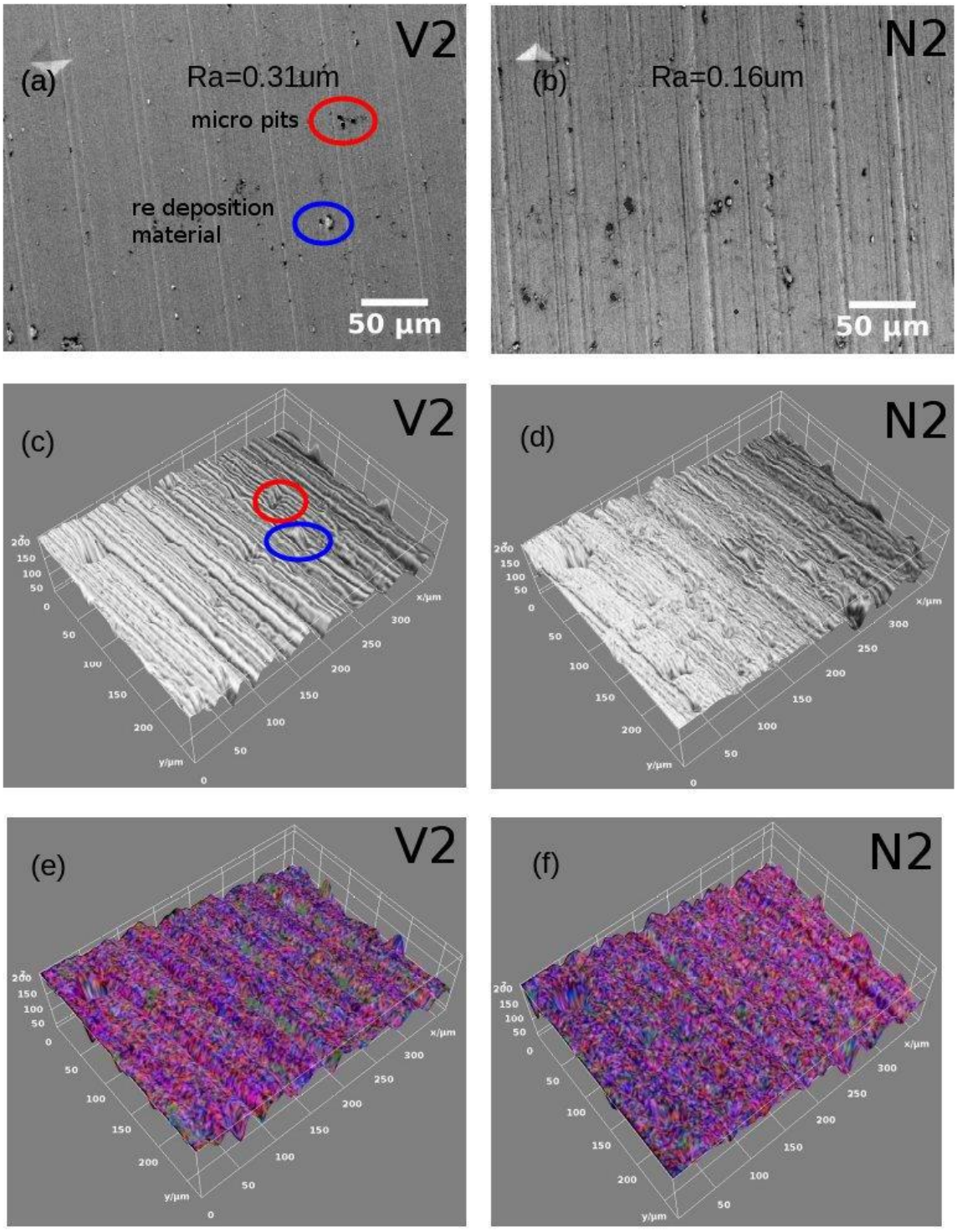

Fig.10 SEM micrographs of machined samples V2 (a) and N2 (b) and equivalent 3D elevation map for V2 (c) and N2 (d) with corresponding EDS map of V2 (e) and N2 (f) for the same cutting parameters: V c=90 m/min; f=0.05 mm/rev; a p=0.5 mm. The red, blue, green, color are representing, respectively, the distribution of Ti, V(e) or Nb (f), and Al.

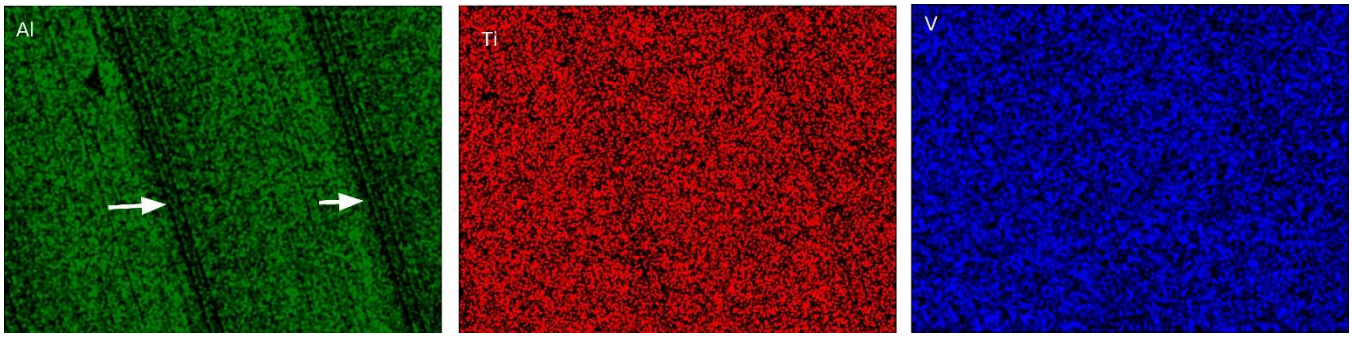

Fig.11. EDS maps from the machined surface of Ti-6Al-4V corresponding Fig.9e. Arrows point to feed marks.

4. Conclusions

Surface topography of dual-phase (α+β) titanium alloys: Ti-6Al-4V and Ti-6Al-7Nb, turned under different cutting conditions, were comparatively analyzed through digital microscopy approaches and roughness descriptors: Ra, Rt and Rz. An innovative approach, the correlative microscopy, has been proposed for inspection of machined surfaces. β phase content in matrix α of both alloys was analyzed quantitatively in terms of volume fraction and distribution homogeneity. The global results of the work allow one to infer that:

- Quantification of microstructural features in Ti-6Al-4V and Ti-6Al-7Nb by digital image analysis confirmed that volume fraction of β phase in Ti-6Al-4V alloy is higher (17%) compared to the volume fraction of β phase in Ti-6Al-7Nb alloy (11%). In addition, Ti-6Al-4V clearly presents a more homogeneously distributed β phase dispersion;

-Cutting conditions influence the topographies and surface microstructures of the biomedical alloys Ti-6Al-4V and Ti-6Al-7Nb. Combination of higher feed rate and lower velocity, V1, produce rougher topography for both alloys, beyond to modify the distribution of chemical elements for Ti-6Al-4V alloy, while the topographic formation obtained by the combination of lower feed rate and higher velocity, V2, seems smoother;

-Ti-6Al-4V presented worse (rougher) surface topography compared to Ti-6Al-7Nb for all tested cutting conditions. This is probably related to the higher volume fraction of β phase in the matrix α phase, since these factors may favor the increase of the mechanical strength in the material. Besides, the results obtained by correlative microscopy showed that the cutting condition V1 produced changes in the homogeneity of the distribution of the chemical elements present in this alloy related to the feed mark patterns;

- There was a qualitative agreement between the global results of the topographic analysis and the values presented by the roughness descriptors, Ra, Rt and Rz;
-The correlative microscopy showed to be an advantageous method to evaluate the surface integrity of the studied biomedical alloys. This technique provides a comprehensive interpretation of the aspects that influence the formation of the surface, by associating the cutting conditions of the machined surfaces with the microstructural factors studied, through the inspection of the surface topography;
-Overall, the current results alone, however, provide some evidence that the Ti-6Al-7Nb is a promising replacement candidate of Ti-6Al-4V, traditionally used.

Acknowledgements

The authors acknowledge “Project No. 031556-FCT/02/SAICT/2017; FAMASI— Sustainable and intelligent manufacturing by machining, financed by the Foundation for Science and Technology (FCT), POCI, Portugal, in the scope of TEMA, Centre for Mechanical Technology and Automation – UID/EMS/00481/2013. The authors also acknowledge TiFast S.R.L., from Italy, for providing the Ti alloys.

Declarations

Ethical Approval

Not applicable

Consent to Participate

Not applicable

Consent to Publish

Not applicable

Authors Contributions

Manuscript title: Surface topography in machining Ti alloys for biomedical applications:
Correlative microscopy approach for qualitative and quantitative analysis All persons who meet authorship criteria are listed as authors, and all authors certify that they have participated sufficiently in the work to take public responsibility for the content, including participation in the conceptualization, methodology, analysis, writing of the manuscript. Furthermore, each author certifies that this material or similar material has not been and will not be submitted to or published in any other publication before its appearance in Advanced Manufacturing Technology.
Authorship specific contributions
Sílvia Carvalho: Experimental work, Ana Horovistiz: Conceptualization, Methodology, Writing - Original Draft preparation. J. Paulo Davim: Conceptualization, Supervision.

Funding

No funding was received to assist with the preparation of this manuscript.

Conflicts of interest/Competing interests

The authors have no relevant financial or non-financial interests to disclose.

Availability of data and materials

The data supporting the article's conclusions are included in the article.

References

[1] Lauro CH, Ribeiro Filho SLM, Brandão LC, Davim JP (2016) Analysis of behaviour biocompatible titanium alloy (Ti-6Al-7Nb) in the micro-cutting. Meas J Int Meas Confed 93:529–540. https://doi.org/10.1016/j.measurement.2016.07.059

[2] Costa BC, Tokuhara CK, Rocha LA, Oliveira LC, Lisboa-Filho PN, Pessoa JC (2019) Vanadium ionic species from degradation of Ti-6Al-4V metallic implants: In vitro cytotoxicity and speciation evaluation. Mater Sci Eng C 96:730–739. https://doi.org/10.1016/j.msec.2018.11.090

[3] Hu HY, Zhang L, He ZY, Jing YH, Tan J (2019) Microstructure evolution, mechanical properties, and enhanced bioactivity of Ti-13Nb-13Zr based calcium pyrophosphate composites for biomedical applications. Mater Sci Eng C 98:279–287. https://doi.org/10.1016/j.msec.2018.12.137

[4] Fellah M, Labaïz M, Assala O, Dekhil L, Taleb A, Rezag H, Iost A (2014) Tribological behavior of Ti-6Al-4V and Ti-6Al-7Nb Alloys for Total Hip Prosthesis. Adv Tribol 2014:1–13. https://doi.org/10.1155/2014/451387

[5] Kara F, Karabatak M, Ayyildiz M, Nas E (2020) Effect of machinability, microstructure and hardness of deep cryogenic treatment in hard turning of AISI D2 steel with ceramic cutting. J Mater Res Technol 9:969–983. https://doi.org/10.1016/j.jmrt.2019.11.037

[6] Padhye NM, Bhange PD, Khimani S (2018) Implant Surface Characteristics and Effects on Osseointegration – A Review. World J Adv Sci Res 1–12

[7] Barfeie A, Wilson J, Rees J (2015) Implant surface characteristics and their effect on osseointegration. Br Dent J 218:1–9. https://doi.org/10.1038/sj.bdj.2015.171

[8] Patil S, Kekade S, Phapale K, Jadhav S, Powar A, Supare A, Singh R (2016) Effect of α and β Phase Volume Fraction on Machining Characteristics of Titanium Alloy Ti6Al4V. Procedia Manuf 6:63–70. https://doi.org/10.1016/j.promfg.2016.11.009

[9] Gangireddy S (2018) Effect of Initial Microstructure on High-Temperature Dynamic Deformation of Ti-6Al-4V Alloy. Metall Mater Trans A Phys Metall Mater Sci 49:4581–4594. https://doi.org/10.1007/s11661-018-4774-1

[10] Rotella G, Dillon OW, Umbrello D, Settineri L, Jawahir IS (2014) The effects of cooling conditions on surface integrity in machining of Ti6Al4V alloy. Int J Adv Manuf Technol 71:47–55. https://doi.org/10.1007/s00170-013-5477-9

[11] Sartori S, Pezzato L, Dabalà M, Maurizi ET, Mertens A, Ghiotti A, Bruschi S (2018) Surface Integrity Analysis of Ti6Al4V After Semi-finishing Turning Under Different Low-Temperature Cooling Strategies. J Mater Eng Perform 27:4810–4818. https://doi.org/10.1007/s11665-018-3598-x

[12] Sun Y, Huang B, Puleo DA, et al (2016) Improved Surface Integrity from Cryogenic Machining of Ti-6Al-7Nb Alloy for Biomedical Applications. Procedia CIRP 45:63–66. https://doi.org/10.1016/j.procir.2016.02.362

[13] Sun SJ, Brandt M, Mo JPT (2013) Effect of Microstructure on Cutting Force and Chip Formation during Machining of Ti-6Al-4V Alloy. Adv Mater Res 690–693:2437–2441. https://doi.org/10.4028/www.scientific.net/AMR.690-693.2437

[14] Berzosa F, Rubio EM, Agustina B, Paulo Davim J (2020) Geometric optimization of drills used to repair holes in magnesium aeronautical components. Metals (Basel) 10:1–21. https://doi.org/10.3390/met10111534

[15] Grzesik W (2016) Prediction of the Functional Performance of Machined Components Based on Surface Topography: State of the Art. J Mater Eng Perform 25:4460–4468. https://doi.org/10.1007/s11665-016-2293-z

[16] Horovistiz A, Laranjeira S, Davim JP (2019) 3-D reconstruction by extended depth-of-field in tribological analysis: Fractal approach of sliding surface in Polyamide66 with glass fiber reinforcement. Polym Test 73:178–185. https://doi.org/10.1016/j.polymertesting.2018.11.017

[17] Hein LRO, Oliveira JA, Campos KA (2013) Correlative fractography: Combining scanning electron microscopy and light microscopes for qualitative and quantitative analysis of fracture surfaces. Microsc Microanal 19:496–500. https://doi.org/10.1017/S1431927612014249

[18] Hein LRO, Campos KA, Caltabiano PCRO, Kostov KG (2013) A Brief Discussion About Image Quality and SEM Methods for Quantitative Fractography of Polymer Composites. Scanning 35:196–204. https://doi.org/10.1002/sca.21048

[19] Obondo BO, Nyangoye BO (2019) Microscopy simple or advance technique of material characterization. Open Sci J 4:1–8. https://doi.org/10.23954/osj.v4i1.2175

[20] Horovistiz A, Carvalho S, Festas AJ, Davim JP (2020) Correlative microscopy analysis of surface topography in machining Ti-6Al-7Nb. Procedia CIRP 88:565–569. https://doi.org/10.1016/j.procir.2020.05.098

[21] Joshi S, Pawar P, Tewari A, Joshi S (2014) Effect of β phase fraction in titanium alloys on chip segmentation in their orthogonal machining. CIRP J Manuf Sci Technol 7:191–201. https://doi.org/10.1016/j.cirpj.2014.03.001

[22] Horovistiz A, Muccillo ENS (2011) Quantification of microstructural features in gadolinia-doped ceria containing co-additives by digital image analysis. J Eur Ceram Soc 31:1431–1438. https://doi.org/10.1016/j.jeurceramsoc.2011.02.022

[23] Mahboob Ali MA, Azmi AI, Mohd Khalil AN, Leong KW (2017) Experimental study on minimal nanolubrication with surfactant in the turning of titanium alloys. Int J Adv Manuf Technol 92:117–127. https://doi.org/10.1007/s00170-017-0133-4

[24] Çelik YH, Kilickap E, Güney M (2017) Investigation of cutting parameters affecting on tool wear and surface roughness in dry turning of Ti-6Al-4V using CVD and PVD coated tools. J Brazilian Soc Mech Sci Eng 39:2085–2093. https://doi.org/10.1007/s40430-016-0607-6

[25] Revuru RS, Zhang JZ, Posinasetti NR, Kidd T (2018) Optimization of titanium alloys turning operation in varied cutting fluid conditions with multiple machining performance characteristics. Int J Adv Manuf Technol 95:1451–1463. https://doi.org/10.1007/s00170-017-1299-5

[26] Agrawal NBP, Khan IA, Khan ZA (2016) Effects of Cutting Parameters on Quality of Surface Produced by Machining of Titanium Alloy and Their Optimization. Arch Mech Eng 63:531–548. https://doi.org/10.1515/meceng-2016-0030

[27] Krishnan NM, Davim, JP (2011) Influence of Coolant in Machinability of Titanium Alloy (Ti-6Al-4V). J Surf Eng Mater Adv Technol 01:9–14. https://doi.org/10.4236/jsemat.2011.11002

[28] Pradhan S, Singh S, Prakash C, Królczyk G, Pramanik A, Pruncu CI (2019) Investigation of

machining characteristics ofhard-to-machine Ti-6Al-4V-ELI alloy for biomedical applications. J Mater Res Technol 8:4849–4862. https://doi.org/10.1016/j.jmrt.2019.08.033

[29] Ibrahim GA, Haron CHC, Ghani JA (2009) Surface integrity of ti-6al-4v eli when machined using coated carbide tools under dry cutting condition. Int J Mech Mater Eng 4:191–196

[30] Gupta K, Laubscher RF (2017) Sustainable machining of titanium alloys: A critical review. Proc Inst Mech Eng Part B J Eng Manuf 231:2543–2560. https://doi.org/10.1177/0954405416634278

[31] Yang D, Liu Z (2016) Quantification of Microstructural Features and Prediction of Mechanical Properties of a Dual-Phase Ti-6Al-4V Alloy. Materials (Basel) 9:1–14. https://doi.org/10.3390/ma9080628